Computer Modeling in Engineering & Sciences
DOI:10.32604/cmes.2020.08867
Article

Robust Remaining Useful Life Estimation Based on an Improved Unscented Kalman Filtering Method

Shenkun Zhao, Chao Jiang*, Zhe Zhang and Xiangyun Long

State Key Laboratory of Advanced Design and Manufacturing for Vehicle Body, College of Mechanical and Vehicle Engineering, Hunan University, Changsha, 410082, China
*Corresponding Author: Chao Jiang. Email: jiangc@hnu.edu.cn
Received: 19 October 2019; Accepted: 11 February 2020

Abstract: In the Prognostics and Health Management (PHM), remaining useful life (RUL) is very important and utilized to ensure the reliability and safety of the operation of complex mechanical systems. Recently, unscented Kalman filtering (UKF) has been applied widely in the RUL estimation. For a degradation system, the relationship between its monitored measurements and its degradation states is assumed to be nonlinear in the conventional UKF. However, in some special degradation systems, their monitored measurements have a linear relation with their degradation states. For these special problems, it may bring estimation errors to use the UKF method directly. Besides, many uncertain factors can result in the fluctuations of the estimated results, which may have a bad influence on the RUL estimation method. As a result, a robust RUL estimation approach is proposed in this paper to reduce the errors and randomness of estimation results for this kind of degradation problems. Firstly, an improved unscented Kalman filtering is established utilizing the Kalman filtering (KF) method and a linear adaptive strategy. The linear adaptive strategy is used to adjust its noise term adaptively. Then, the robust RUL estimation is realized by the improved UKF. At last, three problems are investigated to demonstrate the effectiveness of the proposed method.

Keywords: Remaining useful life; unscented Kalman filtering; state space model

1 Introduction

Due to the importance of reliable and safe operation of complex mechanical systems, more and more researches have been conducted on the Prognostics and Health Management (PHM) in recent years [1–4]. The key points of PHM are condition state assessments and remaining useful life (RUL) estimations [5]. For a running system, its RUL is defined as the period from the current moment to the end of its useful life. In order to give operators the alarms of equipment breakdowns in advance, RUL has been widely applied in many fields, including rotating machinery [6,7], batteries [8,9], aerospace [10], etc.

Many RUL estimation methods have been developed in the past decades [1–6]. In general, the RUL estimation methods can be classified into three categories [11]: the physical-model methods, the data-driven methods and their hybrid. In the physical-model methods, the accurate physical models of degradation processes need to be established to achieve more precise RUL estimations [6]. However, it is often difficult to construct the physical models of complex systems owing to their complicated degradation processes and many uncertain factors [12]. Instead of precise physical models, the data-driven methods utilize condition monitoring data to estimate RUL [1], which seem more convenient for the prognostics of complex systems. The hybrid approach usually represents a combination of the above methods. For the RUL estimation, many difficult problems still exist in practical applications. One of them is the intractable uncertainty caused by limited data, multiple unknown factors and so on [6]. For this reason, more effective methods still need to be explored to deal with the uncertainty in the RUL estimation.

Recently, the stochastic filtering methods have been utilized in both the physics-model and data-driven methods for their ability to tackle uncertainties. The stochastic filtering methods mainly consist of Kalman filtering (KF) [13–15], extended Kalman filtering (EKF) [16–18], unscented Kalman filtering (UKF) [19–21], and particle filtering (PF) [22–24]. KF is the most fundamental filtering method and used only for linear systems [14]. EKF and UKF are developed from KF to deal with nonlinear problems [17,20]. PF solves nonlinearity by the sequential Monte Carlo method [24]. Based on the unscented transform (UT) method, UKF generally can achieve a better estimation accuracy than the EKF [19,25,26]. A key part of PF is the sequential Monte Carlo which requires lots of calculations, so PF usually consume more computations than UKF [27,28]. Due to the reasonable trade-off between computational complexity and capability of handling system nonlinearity, UKF has been widely used and studied for RUL estimations. Chen et al. [29] studied the RUL estimation of the fuel cell in the postal electric vehicles using the UKF method. Dong et al. [30] applied UKF for the remaining dischargeable time estimation of lithium-ion batteries. Tse et al. [31] predicted the remaining useful lives of slurry pumps using the UKF and captured vibration signals. Dolence et al. [32] proposed an integrated approach for the RUL prediction of solid oxide fuel cell stacks based on UKF. Wang et al. [33] studied the UKF for the prognostics of lithium-ion batteries considering heterogeneous noise variances. Cui et al. [34] developed a modified UKF for the RUL prediction of rolling bearing. Zheng et al. [35] researched the RUL estimation of lithium-ion batteries by UKF and relevance vector regression. Daigle et al. [36] conducted a comparison between UKF and PF for the model-based prognostics. Chang et al. [37] explored the RUL estimation of lithium-ion batteries with UKF. Andre et al. [38] proposed a dual filter based on KF and UKF to estimate the internal states of batteries. Wang et al. [39] researched the crack length estimation and propagation with EKF and UKF. Plett [40] investigated UKF for the charge state estimation of Lithium polymer batteries. Zhang et al. [41] presented a UKF-based approach for the remaining discharge energy prediction of the large format lithium-ion battery packs. Santhanagopalan et al. [25] utilized UKF to estimate the state of charge for the high power lithium-ion cells. In the UKF-based methods mentioned above, three main steps can be generally summarized. Firstly, a state space model (SSM) is constructed to represent the degradation process of a given system, consisting of process and measurement equations. Then, after the initialization of the model, the current system state can be estimated using UKF and condition measurements. Finally, the RUL can be predicted for the system based on the current state.

From the above, some UKF-based RUL estimation methods have been developed successfully, however several important factors still need to be considered further in order to achieve more accurate and robust RUL estimations. Firstly, for a degradation system, the relationship between its measurements and its degradation states is currently assume to be nonlinear in the UKF. It should be noticed that practical degradation problems can differ widely from each other. For some special degradation systems, their monitored physical quantities have a linear relation with their degradation states. It may bring estimation errors to use the UKF directly in this special kind of degradation problems. In addition to this, the uncertainties of some initial parameters, such as initial states and initial noise, always exist. Their randomness often influences the estimation results of UKF [42]. Both the aspects mentioned above can have the significant effects on RUL estimations, but little research has been conducted on these. As a result, a robust RUL estimation method is proposed in this work based on an improved unscented Kalman filtering. For the first aspect, an improved unscented Kalman filtering is constructed based on the UKF and KF, in which the KF is used to deal with the linear relationship between the monitored qualities and the degradation states. For the second aspect, an adaptive strategy [43] is utilized in the improved UKF, which can adjust the noise covariance adaptively in the state estimation process. Based on the improved UKF, a robust RUL estimation method is finally conducted. The effectiveness of the proposed RUL estimation method is demonstrated with three engineering problems.

2 The Conventional UKF-Based RUL Estimation

For a degradation system, its RUL is defined as the interval from the current time to the moment when its degradation threshold is reached. With the capability to handle stochastic problems, UKF has been developed and widely used for RUL estimations. In the conventional UKF-based methods [29,30,32,34], there generally exist three basic steps as follows:

Step 1: A state space model (SSM) need to be established to describe the degradation process of a given system as follows [19,26,35]:

$$\begin{cases} \mathbf{x}_k = \mathbf{f}(\mathbf{x}_{k-1}) + \mathbf{w}_k \\ \mathbf{y}_k = \mathbf{h}(\mathbf{x}_k) + \mathbf{v}_k \end{cases} \tag{1}$$

where $\mathbf{f}(\cdot)$ and $\mathbf{h}(\cdot)$ are the process and measurement functions, respectively. k is a time step index. $\mathbf{x}_k$ and $\mathbf{y}_k$ denote the unobserved state and the observed measurement of the degradation process at the time t_k, respectively. The process functions are utilized to describe the degradation process. The measurement functions construct the relationship between the state $\mathbf{x}_k$ and the measurement $\mathbf{y}_k$. $\mathbf{w}_k$ and $\mathbf{v}_k$ are the process and measurement noise terms, respectively. These noise terms represent unknown uncertain factors in the degradation process and are usually set as Gaussian noises, namely $\mathbf{w}_k$ - $N(0, \mathbf{\Sigma}_w)$ and $\mathbf{v}_k$ - $N(0, \mathbf{\Sigma}_v)$.

Step 2: Initialize the initial parameters including: the mean $\hat{\mathbf{x}}_0$ and the covariance $\mathbf{P}_0$ of the initial state $\mathbf{x}_0$, the noise covariances $\mathbf{\Sigma}_w$ and $\mathbf{\Sigma}_v$. Then, with the condition monitoring measurements $[\mathbf{y}_1, \mathbf{y}_2, \ldots, \mathbf{y}_k]$, the means $[\hat{\mathbf{x}}_1, \hat{\mathbf{x}}_2, \ldots, \hat{\mathbf{x}}_k]$ and the covariances $[\mathbf{P}_1, \mathbf{P}_2, \ldots, \mathbf{P}_k]$ of the states $[\mathbf{x}_1, \mathbf{x}_2, \ldots, \mathbf{x}_k]$ at different times can be estimated recursively by UKF [30,32].

Step 3: Based on the estimated states at the current time t_k, the future information of the degradation process can be predicted recursively. If the failure threshold of the system is reached at the time t_m, its RUL can be calculated as the interval between the current time t_k and the predicted failure time t_m, namely, $RUL = t_m - t_k$.

3 Formulation of the Proposed Method

3.1 A Special Kind of Degradation Problems

For some special degradation systems, their nonlinear degradation processes usually can be modeled theoretically in a discrete form as follows:

$$\mathbf{x}_k = \mathbf{f}_{\boldsymbol{\theta}}(\mathbf{x}_{k-1}) \tag{2}$$

where $\boldsymbol{\theta}$ are model parameters. Besides, their monitored quantities $\mathbf{y}_k$ have a linear relation with the degradation state $\mathbf{x}_k$. Considering uncertain factors, this kind of degradation problems can be represented in a discrete form as follows:

$$\mathbf{y}_k = \mathbf{H} \cdot \mathbf{f}_{\boldsymbol{\theta}}(\mathbf{x}_{k-1}) + \boldsymbol{\varepsilon}_k \tag{3}$$

where $\mathbf{H}$ is a matrix. The model parameters $\boldsymbol{\theta}$ are random variables. The noise term $\boldsymbol{\varepsilon}_k$ is a Gaussian noise, namely $\boldsymbol{\varepsilon}_k \sim N(0, \boldsymbol{\Sigma}_\varepsilon)$. Based on Eq. (2), the model in Eq. (3) can be rewritten as follows:

$$\begin{cases} \mathbf{x}_k = \mathbf{f}_{\boldsymbol{\theta}}(\mathbf{x}_{k-1}) \\ \mathbf{y}_k = \mathbf{H} \cdot \mathbf{x}_k + \boldsymbol{\varepsilon}_k \end{cases} \tag{4}$$

The model in Eq. (4) can be seen as a special case of the classical SSM in Eq. (1), and can be solved by the UKF method. However, due to the linear relationship between the monitored quantities with the states, it may bring estimation errors to use the UKF method directly here. In order to obtain more precise and robust estimations for this special case, an improved unscented Kalman filtering is then proposed based on the classical UKF and KF.

3.2 An Improved Unscented Kalman Filtering

In this section, an improved unscented Kalman filtering is founded with the UKF and KF methods for the special degradation problems mentioned above. In the improved UKF method, a linear adaptive strategy [43] is used to adjust the noise term $\mathbf{s}_k$ adaptively to reduce the influence of initial noise parameters. For the special SSM in Eq. (4), the improved UKF algorithm is illustrated in detail as follows:

Step 1: Initialization

According to the history information, the initial parameters should be initialized firstly, including: the mean $\hat{\mathbf{x}}_0$ and covariance $\mathbf{P}_0$ of the initial state $\mathbf{x}_0$ and the initial noise covariance $\boldsymbol{\Sigma}_0$.

Step 2: State prediction at the time t_{k-1}

Based on the information of the state $\mathbf{x}_{k-1}$, the unscented transform (UT) [19] is used to estimate the mean $\hat{\mathbf{x}}_{k|k-1}$ and covariance $\mathbf{P}_{k|k-1}$ of the variable $\mathbf{x}_{k|k-1}$ where $\mathbf{x}_{k|k-1} = \mathbf{f}(\mathbf{x}_{k-1})$. This step includes two sub-steps as follows:

(a) Generate sigma points for the state $\mathbf{x}_{k-1}$

In the UT, the distribution of a Gaussian random variable is represented by a set of sigma points [44,45]. Using the mean $\hat{\mathbf{x}}_{k-1}$ and covariance $\mathbf{P}_{k-1}$ of the state $\mathbf{x}_{k-1}$, $2L+1$ sigma points $\boldsymbol{\chi}_i$ with the corresponding weights W_i are generated to represent the state variable $\mathbf{x}_{k-1}$ through the following equations [46,47]:

$$\begin{cases} \boldsymbol{\chi}_{k-1}^0 = \hat{\mathbf{x}}_{k-1} \\ \boldsymbol{\chi}_{k-1}^i = \hat{\mathbf{x}}_{k-1} + \left(\sqrt{(L+\lambda)\mathbf{P}_{k-1}}\right)_i & i = 1, 2, \ldots, L \\ \boldsymbol{\chi}_{k-1}^i = \hat{\mathbf{x}}_{k-1} - \left(\sqrt{(L+\lambda)\mathbf{P}_{k-1}}\right)_{i-L} & i = L+1, L+2, \ldots, 2L \\ W_0^{(m)} = \lambda/(L+\lambda) \\ W_0^{(c)} = \lambda/(L+\lambda) + (1-\alpha^2+\beta) \\ W_i^{(m)} = W_i^{(c)} = 1/\{2(L+\lambda)\} & i = 1, 2, \ldots, 2L \end{cases} \tag{5}$$

where $\lambda = \alpha^2(L+\kappa) - L$ is a scaling parameter. L is the dimension of the state mean $\hat{\mathbf{x}}_{k-1}$. α is a scaling factor and generally set to 10^{-3}. κ is another scaling parameter and set to $3-L$. β is also a scaling parameter and usually set to 2. $\left(\sqrt{(L+\lambda)\mathbf{P}_{k-1}}\right)_i$ is the ith column of the matrix square root of $(L+\lambda)\mathbf{P}_{k-1}$.

(b) Estimate the mean $\hat{\mathbf{x}}_{k|k-1}$ and covariance $\mathbf{P}_{k|k-1}$

The $2L+1$ sigma points $\boldsymbol{\chi}_{k-1}^i$ are propagated through the nonlinear process functions $f(\cdot)$ as follows:

$$\boldsymbol{\chi}_{k|k-1}^i = \mathbf{f}\left(\boldsymbol{\chi}_{k-1}^i\right) \qquad i = 0, 1, \ldots, 2L \tag{6}$$

Then, the mean $\hat{\mathbf{x}}_{k|k-1}$ and covariance $\mathbf{P}_{k|k-1}$, called the prior information of the state $\mathbf{x}_k$, can be calculated as follows:

$$\begin{cases} \hat{\mathbf{x}}_{k|k-1} = \sum_{i=0}^{2L} W_i^{(m)} \boldsymbol{\chi}_{k|k-1}^i \\ \mathbf{P}_{k|k-1} = \sum_{i=0}^{2L} W_i^{(c)} \left[\boldsymbol{\chi}_{k|k-1}^i - \hat{\mathbf{x}}_{k|k-1} \right] \left[\boldsymbol{\chi}_{k|k-1}^i - \hat{\mathbf{x}}_{k|k-1} \right]^T \end{cases} \tag{7}$$

Step 3: State update at the time t_k

In this step, the mean $\hat{\mathbf{x}}_{k|k-1}$ and covariance $\mathbf{P}_{k|k-1}$ are updated by the measurement data $\mathbf{y}_k$ to obtain the mean $\hat{\mathbf{x}}_k$ and covariance $\mathbf{P}_k$ of the state $\mathbf{x}_k$. Since the measurement equations are linear, this update is carried out through the state update step of KF [48], instead of the classical UKF, as follows [48,49]:

$$\begin{cases} \hat{\mathbf{x}}_k = \hat{\mathbf{x}}_{k|k-1} + \mathbf{K}_k \left[\mathbf{y}_k - \mathbf{H}\hat{\mathbf{x}}_{k|k-1} \right] \\ \mathbf{P}_k = \mathbf{P}_{k|k-1} - \mathbf{K}_k \mathbf{H} \mathbf{P}_{k|k-1} \end{cases} \tag{8}$$

where the matrix $\mathbf{K}_k = \mathbf{P}_{k|k-1} \mathbf{H}^{\mathrm{T}} \left(\mathbf{H} \mathbf{P}_{k|k-1} \mathbf{H}^{\mathrm{T}} + \boldsymbol{\Sigma}_{k-1} \right)^{-1}$ is the Kalman gain matrix. $\boldsymbol{\Sigma}_{k-1}$ is the noise covariance estimation at the time t_{k-1}.

Step 4: Noise covariance adjustment

In order to adjust the noise covariance, the residual-based covariance matching strategy in the adaptive Kalman filtering [43] is applied:

$$\boldsymbol{\Sigma}_k = \mathbf{C}_k + \mathbf{H}\mathbf{P}_k\mathbf{H}^{\mathrm{T}} \tag{9}$$

where $\mathbf{C}_k$ is the sum of a residual sequence:

$$\mathbf{C}_k = \frac{1}{N} \sum_{j=k-N+1}^{k} \mathbf{v}_j \mathbf{v}_j^T \tag{10}$$

where N is a window size parameter, and $\mathbf{v}_j$ is a residual error at the time t_j:

$$\begin{cases} \hat{\mathbf{y}}_j = \mathbf{H}\hat{\mathbf{x}}_j \\ \mathbf{v}_j = \mathbf{y}_j - \hat{\mathbf{y}}_j \end{cases} \tag{11}$$

where $\mathbf{y}_j$ is the measurement data and $\hat{\mathbf{y}}_j$ is the predicted measurement through the estimated mean $\hat{\mathbf{x}}_j$ at the time t_j. If this step is carried out at the beginning of the state estimation process, namely $1 \le k \le N$, the $\mathbf{C}_k$ can be substituted by:

$$\mathbf{C}_k = \frac{1}{k} \sum_{j=1}^{k} \mathbf{v}_j \mathbf{v}_j^T \tag{12}$$

From the above, based on the Steps 2-4 and the measurements $\left[\mathbf{y}_i | i = 1, 2, \ldots, k \right]$, the mean $\hat{\mathbf{x}}_k$ and covariance $\mathbf{P}_k$ of the current state $\mathbf{x}_k$ can be estimated recursively, meanwhile the noise covariance is adjusted adaptively.

3.3 The RUL Estimation

Based on the estimated state $\hat{\mathbf{x}}_k$ at the current time t_k, the future degradation information $\hat{\mathbf{x}}_{k+1}$and $\hat{\mathbf{y}}_{k+1}$ at the time t_{k+1} can be predicted:

$$\begin{cases} \hat{\mathbf{x}}_{k+1} = \mathbf{f}(\hat{\mathbf{x}}_k) \\ \hat{\mathbf{y}}_{k+1} = \mathbf{H} \cdot \hat{\mathbf{x}}_{k+1} + \mathbf{s} \end{cases} \tag{13}$$

where $\mathbf{s} \sim N(0, \boldsymbol{\Sigma}_k)$ is the noise term. Assuming a failure occurs when the degradation process crosses a given failure threshold, the step in Eq. (13) can be carried out recursively until the degradation process reaches the given failure threshold. If $\mathbf{y}_k$ is a one-dimensional measurement, the failure time of the increasing degradation process can be defined as follows:

$$\begin{cases} \hat{y}_{k+r} \le FT \\ \hat{y}_{k+r+1} > FT \\ RUL = t_{k+r} - t_k \end{cases} \tag{14}$$

where $\hat{y}_{k+r}$ and $\hat{y}_{k+r+1}$ are the predicted degradation quantities at the time t_{k+r} and t_{k+r+1}, respectively. FT is a failure threshold and the time t_{k+r} is defined as the failure time, when the degradation quantity hits the failure threshold for the first time. Then, the RUL at the current time t_k is obtained as RUL. If the degradation process is decreasing, its failure time is defined inversely as the time t_{k+r} when $\hat{y}_{k+r} \ge FT$ and $\hat{y}_{k+r+1} < FT$.

In the conventional UKF-based RUL estimation, it is usually difficult to set the initial mean $\hat{\mathbf{x}}_0$ well because of its uncertainty in practice. Instead of a certain value, it may be easy to provide a reasonable initial interval $\left[\hat{\mathbf{x}}_0^L, \hat{\mathbf{x}}_0^U\right]$ for the initial mean $\hat{\mathbf{x}}_0$, namely $\hat{\mathbf{x}}_0 \in \left[\hat{\mathbf{x}}_0^L, \hat{\mathbf{x}}_0^U\right]$. In order to reduce the influence of the uncertainty of $\hat{\mathbf{x}}_0$, M initial samples are generated from its initial interval as its initialization in the following RUL estimation algorithm. In conclusion, the framework of the robust RUL estimation method is exhibited in Fig. 1 and the algorithm is shown in detail as follows:

Step 1: Initialization

After establishing the SSM of a degradation process, the initial parameters can be given by the historical data of same or similar degradation problems, including: the initial mean interval $\left[\hat{\mathbf{x}}_0^L, \hat{\mathbf{x}}_0^U\right]$ and the initial covariance $\mathbf{P}_0$ of the initial state $\mathbf{x}_0$ and the initial noise covariance $\boldsymbol{\Sigma}_0$. Then, M initial samples $\left[\hat{\mathbf{x}}_0^i | i = 1, 2, \ldots, M\right]$ are generated from the interval $\left[\hat{\mathbf{x}}_0^L, \hat{\mathbf{x}}_0^U\right]$ for the initial mean $\hat{\mathbf{x}}_0$. As a result, M initial samples $\left[\left(\hat{\mathbf{x}}_0^i, \mathbf{P}_0, \boldsymbol{\Sigma}_0\right) | i = 1, 2, \ldots, M\right]$ are obtained for the following steps.

Step 2: The current state estimation

Based on the M initial samples, M estimations $\left[\left(\hat{\mathbf{x}}_k^i, \mathbf{P}_k^i, \boldsymbol{\Sigma}_k^i\right) | i = 1, 2, \ldots, M\right]$ of the current state $\mathbf{x}_k$ can be acquired through the improved UKF and the measurements $\left[\mathbf{y}_i | i = 1, 2, \ldots, k\right]$.

Step 3: Future degradation prediction

For each estimations $\left[\left(\hat{\mathbf{x}}_k^i, \mathbf{P}_k^i, \boldsymbol{\Sigma}_k^i\right) | i = 1, 2, \ldots, M\right]$ of the current state $\mathbf{x}_k$, the prediction step in Eq. (13) is carried out recursively until the degradation process reaches the given failure threshold FT.

Step 4: RUL estimation

After the Step 3, M RUL estimations $\left[RUL_i \;|\; \left(\hat{\mathbf{x}}_k^i, \mathbf{P}_k^i, \boldsymbol{\Sigma}_k^i\right), i = 1, 2, \ldots, M\right]$ can be achieved at the current time t_k. Therefore, the distribution information of the RUL can be described based on these M samples, such as the mean, the covariance, the confidence interval and so on.

4 Applications

4.1 The Battery Degradation Problem

The reliability of batteries are more and more important in complex electromechanical systems, such as electric vehicles, airplanes, high-speed rail and so on. However, it is widely known that the capacity of a battery degrades over cycles until its failure threshold is reached. This kind of degradation problem is researched through a battery case [50]. In this case, the capacity degradation process is expressed by an exponential growth model [50] as follows:

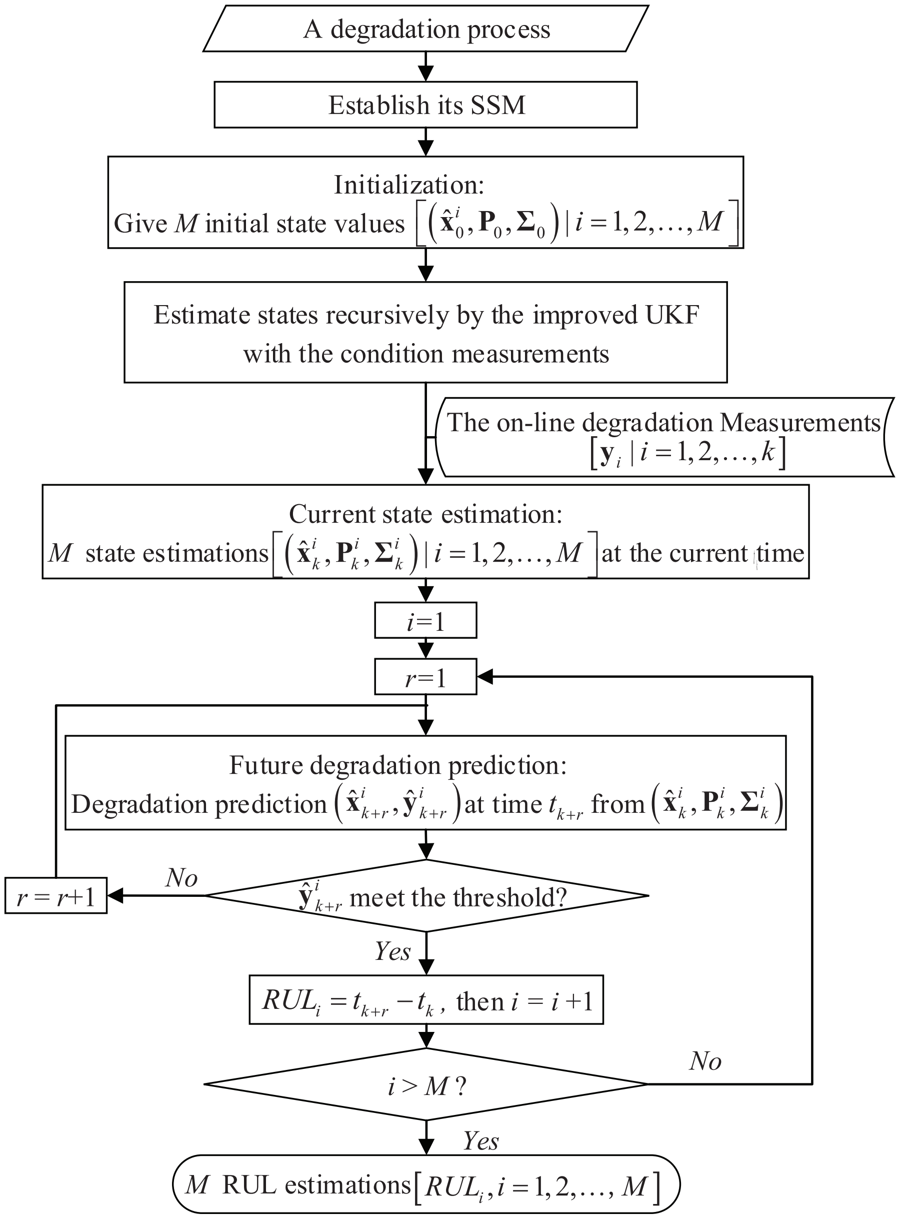

Figure 1: The flowchart of the proposed RUL estimation method

$$C = a\exp(-bt) \tag{15}$$

where a and b are the model parameters, t is the time index, and C is the battery capacity. The capacity data [50] are given at every 5 weeks as shown in Tab. 1. Based on the information (C_{k-1}, b_{k-1}) at the time t_{k-1}, the degradation model can be rewritten in a discrete form as follows:

$$C_k = \exp(-b_{k-1}\Delta t)C_{k-1} \tag{16}$$

where Δt is a time interval between the time t_{k-1} and t_k. C_{k-1} and C_k are the capacity values at the time t_{k-1} and t_k, respectively. b_{k-1} is the estimation of the parameter b at the time t_{k-1}. Then, the SSM of this battery can be constructed as follows:

Table 1: Battery degradation measurement [50]

Time step k	Time (weeks)	Capacity (Ahr)	Time step k	Time (weeks)	Capacity (Ahr)
0	0	1.0000	5	25	0.7114
1	5	0.9351	6	30	0.6830
2	10	0.8512	7	35	0.6147
3	15	0.9028	8	40	0.5628
4	20	0.7754	9	45	0.7090

$$\mathbf{x}_k = \mathbf{f}(\mathbf{x}_{k-1}) \ : \ \begin{cases} C_k = \exp(-b_{k-1}\Delta t)C_{k-1} \\ b_k = b_{k-1} \end{cases} \tag{17}$$

$$y_k = \mathbf{H} \cdot \mathbf{x}_k + \varepsilon_k = C_k + \varepsilon_k \tag{18}$$

where Eqs. (17) and (18) are the process and measurement equations, respectively. $\mathbf{x}_k = [C_k, b_k]$ is the state vector including the capacity C_k and the model parameter b_k at the time t_k. y_k is a capacity measurement. The noise term is a Gaussian noise, namely ε_k - $N\left(0, \sigma_k^2\right)$. The initial parameters are given in Tab. 2. $\hat{C}_0$ and $\hat{b}_0$ of the initial mean $\hat{\mathbf{x}}_0 = \left[\hat{C}_0,\ \hat{b}_0\right]$ are set as intervals. σ_C and σ_b are the initial standard deviations of the initial parameters C_0 and b_0, respectively. $\mathbf{P}_0$ is the initial covariance of the initial state $\mathbf{x}_0$. M is the number of the initial state samples. N is the window size parameter in the improved UKF. FT is the degradation threshold of battery capacity and set as 0.3 [50].

Table 2: The parameter initialization

Parameter	Initial value	Units	Parameter	Initial value	Units
$\hat{C}_0$	[0.9000 1.1000]	Ahr	$\mathbf{P}_0$	$\begin{bmatrix} \sigma_C^2 & 0 \\ 0 & \sigma_b^2 \end{bmatrix}$	/
$\hat{b}_0$	[0.0080 0.0160]	/	M	5000	/
σ_C	0.0577	/	N	9	/
σ_b	0.0023	/	FT	0.3000	Ahr

Based on the capacity measurements, the battery RULs at 45 weeks can be estimated by the filtering methods under different initial noise standard deviations σ_0. The estimation results of the proposed method and the UKF-based method are both given in Tab. 3. The 5, 50 (median) and 95 percentiles of the RUL distribution and its means are estimated through the M RUL estimation samples, in which the estimated mean value takes only integers. The estimated mean RULs of the battery are shown in Fig. 2. The proposed method utilizes an adaptive strategy to adjust the noise variance adaptively and the adjustment process of the noise deviation σ is shown in Fig. 3, in which the noise is estimated and updated gradually to the true value during the state estimation process. For the estimated RUL, M estimated RUL samples are used to describe its distribution, and the histogram of the RUL by the samples is shown in Fig. 4. In the proposed method, the state space model of the battery is updated firstly by the monitoring measurement. Then the capacities of the battery is predicted at each time by the updated model to estimate RUL. The diagram of the capacity prediction is shown in Fig. 5, in which M estimated samples of the battery capacity is used to represent its distribution at each time.

Table 3: RUL (weeks) prediction at 45 weeks under different initial noise standard deviations

Method	RUL percentiles			Mean RUL	Real RUL	σ_0
	5prct	Median	95prct			
The proposed method	40	55	70	53	55	0.02
	40	55	70	53	55	0.03
	40	55	70	53	55	0.04
	40	55	70	53	55	0.05
	35	55	70	53	55	0.06
	35	55	70	53	55	0.07
	35	55	70	53	55	0.08
	35	55	70	53	55	0.09
	35	55	70	53	55	0.10
The UKF-based method	50	60	70	60	55	0.02
	45	60	70	58	55	0.03
	40	55	70	55	55	0.04
	35	55	70	52	55	0.05
	30	50	70	50	55	0.06
	25	45	70	47	55	0.07
	25	45	70	44	55	0.08
	20	40	65	42	55	0.09
	15	40	65	40	55	0.10

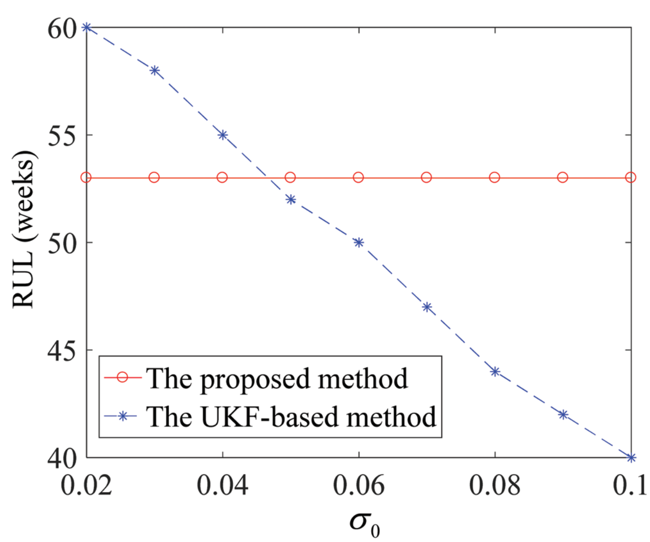

Figure 2: The mean RULs estimated by the proposed method and the UKF-based method under different initial noise deviations σ_0

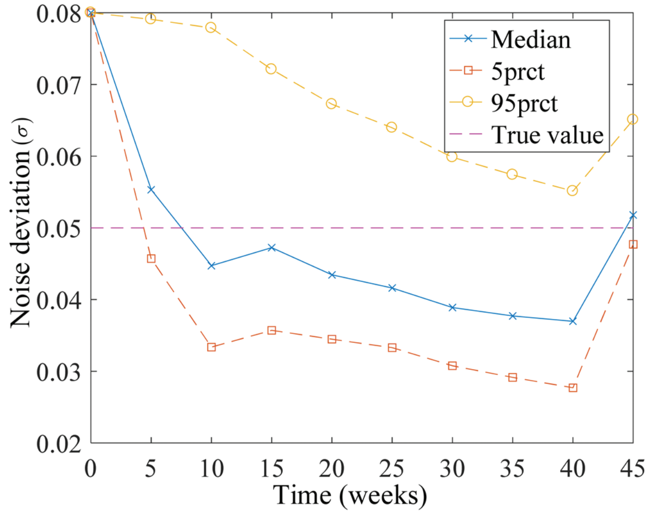

Figure 3: The adjustment process of the noise deviation σ in the proposed method ($\sigma_0 = 0.08$)

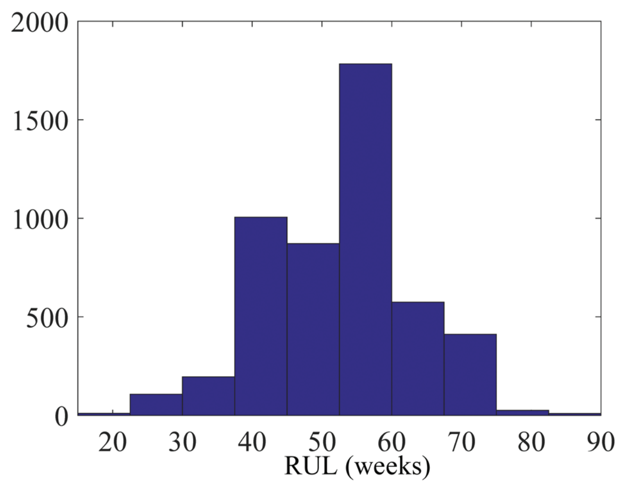

Figure 4: The histogram of the RUL at 45 weeks estimated by the proposed method ($\sigma_0 = 0.08$)

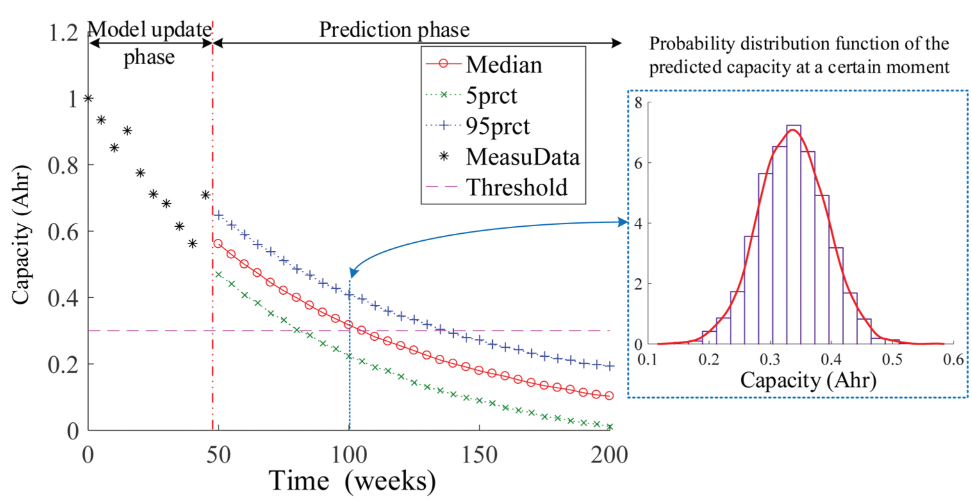

Figure 5: The capacity prediction of the battery at 45 weeks by the proposed method ($\sigma_0 = 0.08$)

4.2 The Electrolytic Capacitor Degradation Problem

Electrolytic capacitors are also very critical components in many electromechanical systems, but they are known for low reliability and frequent breakdowns in the practical systems [51]. In this case, the prognostics of electrolytic capacitors are analyzed through a dataset from the NASA Ames Prognostics Data Repository [52]. In this dataset, six commercial capacitors were subjected to electrical overstress in order to observe and record their degradation processes, referring to Refs. [51,52] for the further details of the experiments and dataset. For a capacitor, its internal degradation results in the gradual increase of its resistance and the gradual decrease of its capacitance over time. The percentage capacitance loss is mostly selected as a degradation indicator to represent the degradation process, as shown in the Fig. 6. Considering the relevant research [51], an empirical degradation model of this capacitor is utilized as follows:

$$C_l(t) = \exp(\alpha \cdot t) + \beta \tag{19}$$

where $C_l(t)$ is the percentage loss of this capacitance at the time t. α and β are the degradation model parameters. Based on the information $(C_l^{k-1},\ \alpha_{k-1},\ \beta_{k-1})$ at the time t_{k-1}, the degradation model can be rewritten in a discrete form as follows:

$$C_l^k = \exp(\alpha_{k-1}\Delta t_k) \cdot \left(C_l^{k-1} - \beta_{k-1}\right) + \beta_{k-1} \tag{20}$$

where C_l^k and C_l^{k-1} are the percentage capacitance loss at the time t_k and t_{k-1}, respectively. Δt_k is a time interval between the time t_{k-1} and t_k. α_{k-1} and β_{k-1} are the estimations of the parameters α and β at the time t_{k-1}, respectively. Then, the SSM for this capacitor can be constructed as follows:

$$\mathbf{x}_k = \mathbf{f}(\mathbf{x}_{k-1}) : \begin{cases} C_l^k = \exp(\alpha_{k-1}\Delta t_k) \cdot \left(C_l^{k-1} - \beta_{k-1}\right) + \beta_{k-1} \\ \alpha_k = \alpha_{k-1} \\ \beta_k = \beta_{k-1} \end{cases} \tag{21}$$

$$y_k = \mathbf{H} \cdot \mathbf{x}_k + \varepsilon_k = C_l^k + \varepsilon_k \tag{22}$$

where Eqs. (21) and (22) are the process and measurement equations, respectively. $\mathbf{x}_k = \left[C_l^k,\ \alpha_k,\ \beta_k\right]$ is the state vector at the time t_k including the percentage capacitance loss C_l^k, the model parameters α_k and β_k. y_k is the percentage capacitance loss measurement. The noise term ε_k obeys a Gaussian noise $N\left(0,\ \sigma_k^2\right)$. The sixth capacitor is selected as the predicted object and its measurements are shown in Tab. 4. The initialization of

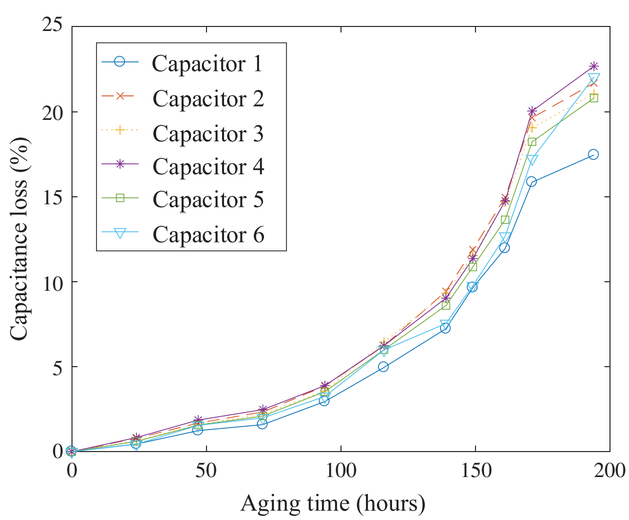

Figure 6: Degradation of capacitor performance

the parameters in the RUL estimation method is given in Tab. 5. $\hat{C}_l^0$, $\hat{\alpha}_0$ and $\hat{\beta}_0$ of the initial mean $\hat{\mathbf{x}}_0 = \left[\hat{C}_l^0,\ \hat{\alpha}_0,\ \hat{\beta}_0\right]$ are set as intervals. σ_C, σ_α and σ_β are the standard deviations of the initial parameters C_l^0, α_0 and β_0, respectively. $\mathbf{P}_0$ is the initial covariance of the initial state $\mathbf{x}_0$. FT is a threshold for the percentage capacitance loss (%), which is set as 20 [51].

With the measurements of the capacitor, its RULs at 171 h are predicted by the filtering methods under different initial noise standard deviations σ_0. The prediction results are shown in Tab. 6. The estimated mean RULs of the capacitor are shown in Fig. 7. The histogram of the predicted RUL by the estimated RUL samples is shown in Fig. 8. The diagram of the capacitance loss prediction of the capacitor is shown in Fig. 9, in which M estimated samples of the capacitance loss is used to describe its distribution at each time.

Table 4: Capacitor degradation measurement [52]

Time step k	Time (h)	Capacitance loss (%)	Time step k	Time (h)	Capacitance loss (%)
0	0	0	5	116	5.990
1	24	0.442	6	139	7.540
2	47	1.550	7	149	9.760
3	71	1.990	8	161	12.680
4	94	3.250	9	171	17.230

Table 5: The parameter initialization

Parameter	Initial value	Units	Parameter	Initial value	Units
$\hat{C}_l^0$	[0 0.400]	/	σ_C	0.030	/
$\hat{\alpha}_0$	[0.013 0.023]	/	σ_α	0.002	/
$\hat{\beta}_0$	[-0.570 -0.470]	/	σ_β	0.010	/
M	5000	/	$\mathbf{P}_0$	$\begin{bmatrix} \sigma_C^2 & 0 & 0 \\ 0 & \sigma_\alpha^2 & 0 \\ 0 & 0 & \sigma_\beta^2 \end{bmatrix}$	/
N	5	/			
FT	20.000	/			

4.3 The Milling Tool Degradation Problem

For the inserts of tools in a milling machine, milling insert wear can arise from the abrasion of the hard constituents in work piece material [53]. Once the wear on the inserts exceeds a standard threshold level, the tools are considered to be disabled. The milling tool degradation is researched through a dataset from the NASA Ames Prognostics Data Repository [54,55]. This dataset contains sixteen cases running on a Matsuura machining center MC-510V under different speeds, feeds, and depth of cut. A 70 mm face mill with 6 inserts (KC710) is chosen as the tool in the dataset, as shown in Fig. 10. The interaction between work pieces and milling tools can result in different kinds of tool wear. In these experiments, the flank wear VB is selected to evaluate the tool wear [55], as shown in Fig. 11. The VB measurements of the 3th case in the dataset are shown in Fig. 12. Considering the changing tendency of the flank wear VB, an empirical degradation model is founded on an exponential growth model as follows:

$$W(t) = c \cdot \exp(a \cdot t) + b \tag{23}$$

Table 6: RUL (h) prediction of capacitor at 171 h under different initial noise standard deviations

Method	RUL percentiles			Mean RUL	Real RUL	σ_0
	5prct	Median	95prct			
The proposed method	9	12	14	11	13	0.05
	9	12	15	11	13	0.10
	9	12	15	11	13	0.50
	9	12	15	11	13	0.70
	9	12	15	11	13	0.90
	9	12	15	11	13	1.10
	9	12	15	11	13	1.30
	9	12	15	11	13	1.50
	9	12	15	11	13	1.70
	9	12	15	11	13	1.90
	9	12	15	11	13	2.10
The UKF-based method	10	11	11	10	13	0.05
	10	11	12	11	13	0.10
	9	12	15	11	13	0.50
	8	11	15	11	13	0.70
	7	11	14	10	13	0.90
	6	10	14	10	13	1.10
	5	10	14	9	13	1.30
	4	9	14	9	13	1.50
	3	9	14	8	13	1.70
	2	8	14	8	13	1.90
	2	8	14	7	13	2.10

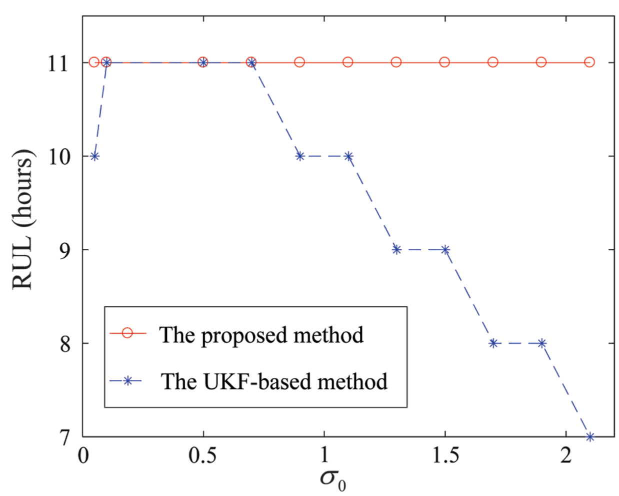

Figure 7: The mean RULs estimated by the proposed method and the UKF-based method under different initial noise deviations σ_0

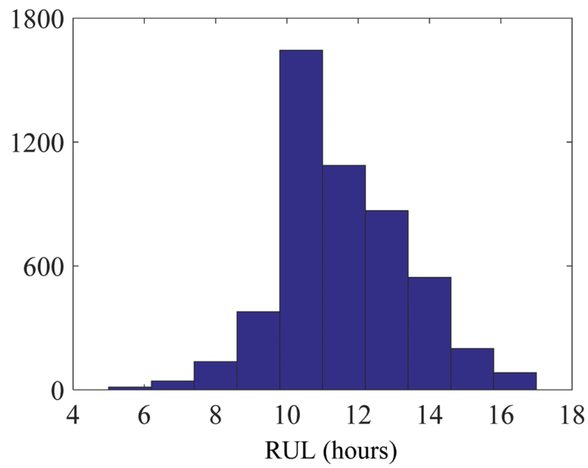

Figure 8: The histogram of the estimated RUL at 171 h by the proposed method ($\sigma_0 = 1.1$)

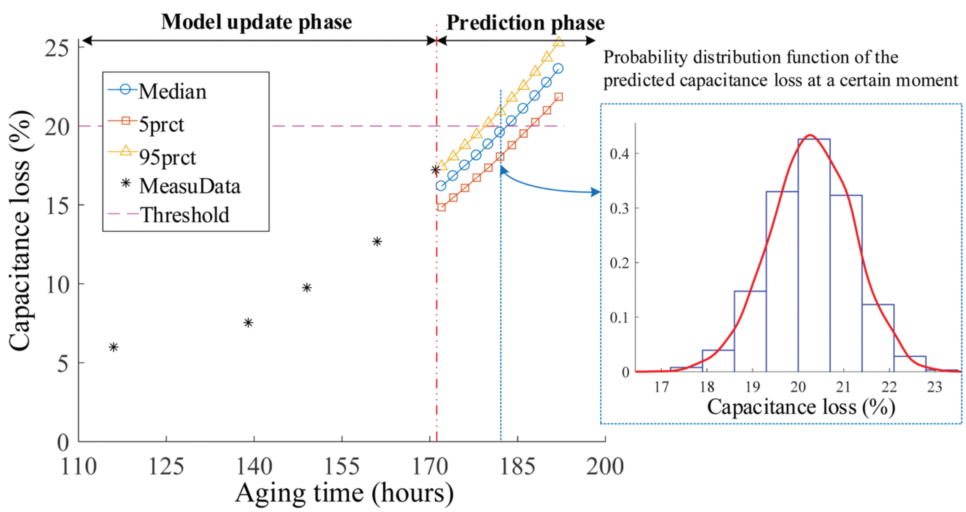

Figure 9: The capacitor degradation prediction at 171 h by the proposed method ($\sigma_0 = 1.1$)

where $W(t)$ represents the flank wear VB at the time t. a, b and c are the model parameters. Based on the information (W_{k-1}, a_{k-1}, b_{k-1}) at the time t_{k-1}, the degradation model can be rewritten in a discrete form as follows:

$$W_k = \exp(a_{k-1} \cdot \Delta t_k) \cdot (W_{k-1} - b_{k-1}) + b_{k-1} \tag{24}$$

where W_k and W_{k-1} are the flank wear at the time t_k and t_{k-1}, respectively. a_{k-1} and b_{k-1} are the estimations of the parameter a and b at the time t_{k-1}. Then, the SSM of the milling tool degradation can be constructed as follows:

$$\mathbf{x}_k = \mathbf{f}(\mathbf{x}_{k-1}): \begin{cases} W_k = \exp(a_{k-1}\Delta t_k) \cdot (W_{k-1} - b_{k-1}) + b_{k-1} \\ a_k = a_{k-1} \\ b_k = b_{k-1} \end{cases} \tag{25}$$

$$y_k = \mathbf{H} \cdot \mathbf{x}_k + \varepsilon_k = W_k + \varepsilon_k \tag{26}$$

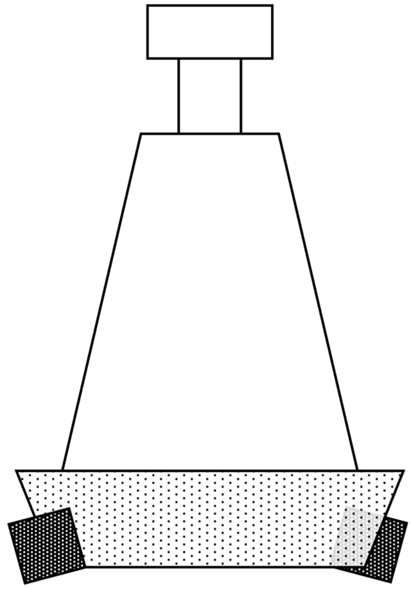

Figure 10: Schematic of the tool and inserts of the face mill [55]

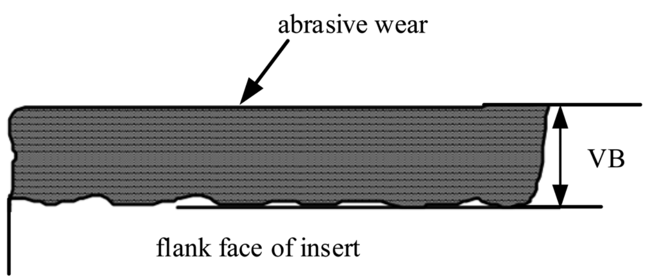

Figure 11: Tool wear VB as it is seen on the insert [55]

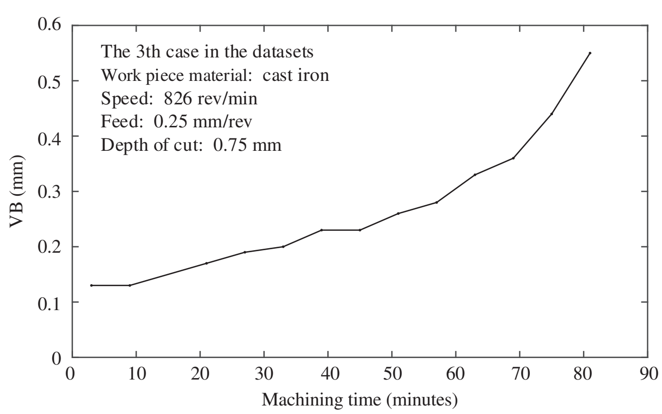

Figure 12: Tool wear VB over time

where $\mathbf{x}_k = [W_k, a_k, b_k]$ is the state vector at the time t_k. Eqs. (25) and (26) represent the process and measurement equations, respectively. y_k is the flank wear VB measurement at the time t_k. The noise term ε_k follows a Gaussian noise $N\left(0,\ \sigma_k^2\right)$. The eleventh case in the dataset is selected as the object to be predicted. Its experiment conditions and the flank wear VB measurements are shown in Tabs. 7 and 8, respectively. The initialization of the parameters in the estimation method is given in Tab. 9. $\hat{\mathbf{x}}_0 = \left[\hat{W}_0, \hat{a}_0, \hat{b}_0\right]$ is the initial mean of the initial state $\mathbf{x}_0 = [W_0, a_0, b_0]$, in which $\hat{W}_0$, $\hat{a}_0$ and $\hat{b}_0$ are set as intervals. σ_W, σ_a and σ_b represent the standard deviations of the initial parameters W_0, a_0 and b_0, respectively. $\mathbf{P}_0$ is the initial covariance of the initial state $\mathbf{x}_0$. FT is a threshold for the flank wear VB, which is set as 0.76 mm.

Table 7: Experimental condition [55]

Case	Depth of Cut (mm)	Feed (mm/rev)	Cutting speed (rev/min)	Work piece material
11	0.75	0.25	826	cast iron

Table 8: Flank wear VB measurement [55]

Time step k	Time (min)	VB (mm)	Time step k	Time (min)	VB (mm)
0	0	0	8	33	0.18
1	3	0.04	9	39	0.20
2	10	0.07	10	45	0.23
3	12	0.07	11	51	0.26
4	14	0.08	10	57	0.31
5	17	0.09	13	63	0.37
6	21	0.12	14	72	0.42
7	27	0.16	15	80	0.47

Table 9: The parameter initialization

Parameter	Initial value	Units	Parameter	Initial value	Units
$\hat{W}_0$	[0, 0.080]	mm	σ_W	0.020	/
$\hat{a}_0$	[0.014, 0.024]	/	σ_a	0.002	/
$\hat{b}_0$	[-0.062, -0.052]	/	σ_b	0.002	/
M	5000	/	$\mathbf{P}_0$	$\begin{bmatrix} \sigma_W^2 & 0 & 0 \\ 0 & \sigma_a^2 & 0 \\ 0 & 0 & \sigma_b^2 \end{bmatrix}$	/
N	15	/			
FT	0.760	mm			

Based on the measurements of the milling tool, its RULs at 80 min are predicted by the filtering methods under different initial noise standard deviations σ_0. The RUL estimated results are given in Tab. 10. The estimated mean RULs of the milling tool are shown in Fig. 13. The histogram of the RUL by the estimated RUL samples is shown in Fig. 14. The diagram of the tool wear prediction is shown in Fig. 15, in which the distribution of the tool wear at each time is predicted by its M estimated samples.

Table 10: RUL (min) prediction of Mill Tool at 80 min under different initial noise standard deviations

Method	RUL percentiles			Mean RUL	Real RUL	σ_0
	5prct	Median	95prct			
The proposed method	18	20	22	20	25	0.02
	18	21	23	20	25	0.04
	18	21	23	20	25	0.06
	18	21	23	20	25	0.08
	18	21	23	20	25	0.10
	18	21	23	20	25	0.12
	18	21	23	20	25	0.14
	18	21	23	20	25	0.16
	18	21	23	20	25	0.18
The UKF-based method	18	20	22	19	25	0.02
	14	19	23	18	25	0.04
	11	17	25	17	25	0.06
	8	16	26	16	25	0.08
	5	15	27	15	25	0.10
	3	13	28	14	25	0.12
	2	12	28	12	25	0.14
	2	10	28	11	25	0.16
	1	9	28	10	25	0.18

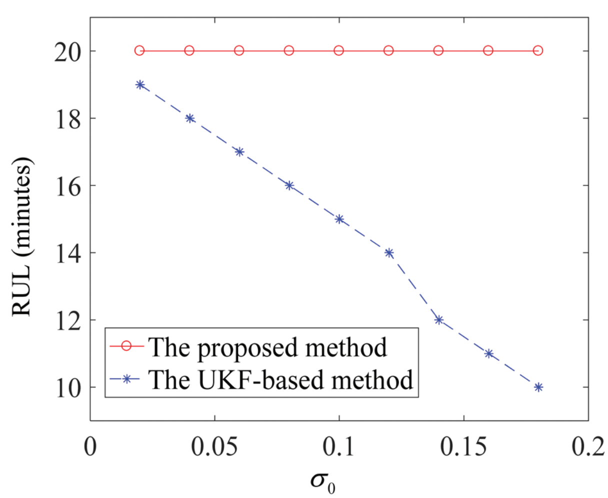

Figure 13: The mean RULs estimated by the proposed method and the UKF-based method under different initial noise deviations σ_0

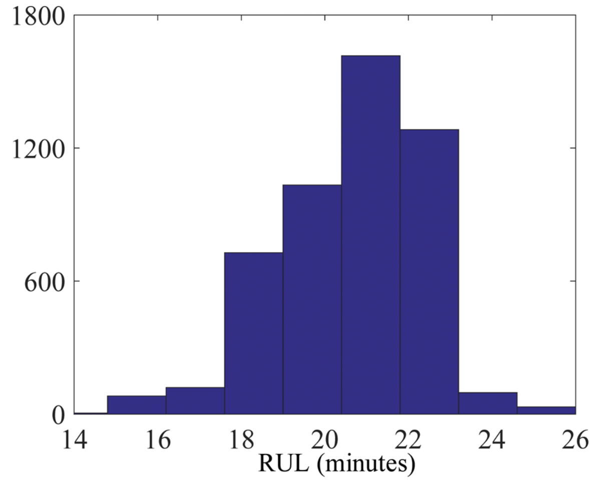

Figure 14: The histogram of the estimated RUL at 80 min by the proposed method ($\sigma_0 = 0.10$)

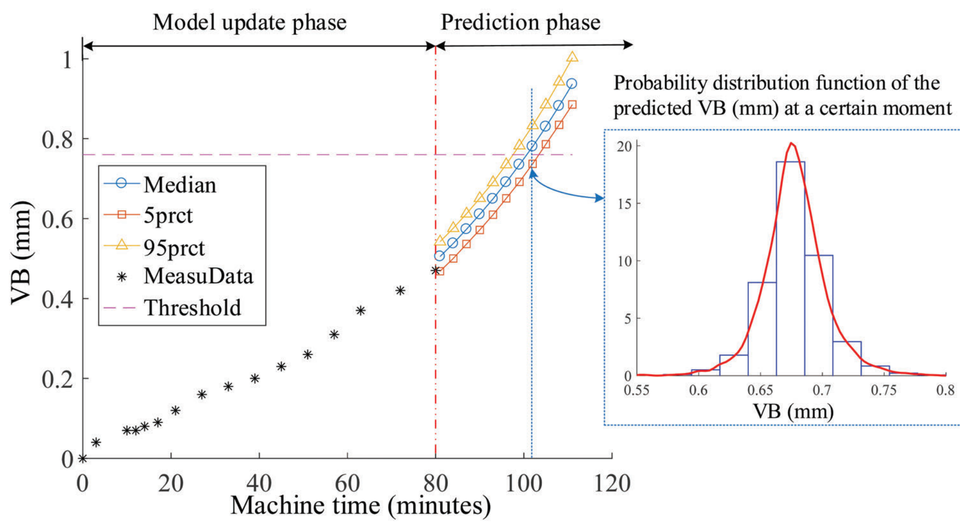

Figure 15: The tool wear prediction at 80 min by the proposed method ($\sigma_0 = 0.10$)

4.4 Analysis of the Results

The results of the three applications are shown in the above. By comprehensively analyzing the results, we can find the following points:

1. Robustness. The mean of the RUL distribution is utilized as the estimated point to verify the robustness of the proposed method, as shown in Tab. 12. Under different initial noise standard deviations, the estimated RUL results of the proposed method remain stable with no fluctuation, which is shown in Tab. 12 and Figs. 2, 7 and 13. However, the RUL results of the conventional UKF-based method are fluctuant under the same conditions in the three cases, and their fluctuation intervals are [40.0, 60.0], [7.0, 11.0] and [10.0, 19.0], respectively. This is because an adaptive strategy is utilized in the proposed method to adjust the noise variance adaptively during the state estimation process as shown in Fig. 3. For different number of initial samples, the fluctuation of the estimated results of the proposed method is analyzed in Tab. 11, in which the method is tested 10 times. When the number is 500 or 1000, the 5 percentiles of the RUL distributions fluctuate in [35,40], [8,9], and [17,18] in the three cases,

respectively. The mean of the estimated RUL fluctuates in [52,54] in Case 1. With the increase of the number, the proposed method remains stable with no fluctuation when the number is 3000 or 5000. Therefore, the estimated RUL results of the proposed method can remain stable under the uncertain parameters.

2. Accuracy. The mean RUL is also utilized as the estimated point to verify the accuracy of the proposed method as shown in Tab. 12. The estimation error is defined as the absolute value between the estimated point and the real RUL. A smaller average error means a more accurate estimation. In the analyzed cases, the average errors of the estimated results by the proposed method are 2.0, 2.0 and 5.0, respectively. The average errors of the UKF-based method are 7.0, 3.5, and 10.3, respectively, which are greater than the errors of the proposed method. The results show that the proposed method can achieve more accurate RUL estimations.
3. To sum up, the proposed approach can reduce the randomness of its results and provide relatively robust and accurate RUL estimations from the above analysis of three cases. In practice, fluctuant estimated RULs may cause a difficulty for operators to make a proper maintenance plan, and the stable results can reduce this influence. As a result, the proposed robust approach seems a useful tool in the RUL estimation for many engineering problems.

Table 11: Fluctuation of the proposed method by test 10 times under different number of initial samples

	RUL percentiles			Mean RUL	Number
	5prct	Median	95prct		
Case 1	[35, 40]	55	70	[52, 54]	500
	[35, 40]	55	70	[52, 54]	1000
	35	55	70	53	3000
	35	55	70	53	5000
Case 2	[8, 9]	12	15	11	500
	[8, 9]	12	15	11	1000
	9	12	15	11	3000
	9	12	15	11	5000
Case 3	[17, 18]	21	23	20	500
	[17, 18]	21	23	20	1000
	18	21	23	20	3000
	18	21	23	20	5000

Table 12: Comparison of RUL estimations under different initial noise standard deviations in the three cases

	Method	Fluctuation of mean RUL	Real RUL	Error range	Average error
Case 1	The proposed method	[53.0, 53.0]	55	[2.0, 2.0]	2.0
	UKF-based method	[40.0, 60.0]	55	[0.0, 15.0]	7.0
Case 2	The proposed method	[11.0, 11.0]	13	[2.0, 2.0]	2.0
	UKF-based method	[7.0, 11.0]	13	[2.0, 6.0]	3.5
Case 3	The proposed method	[20.0, 20.0]	25	[5.0, 5.0]	5.0
	UKF-based method	[10.0, 19.0]	25	[6.0, 15.0]	10.3

5 Conclusions

In order to achieve robust and accurate RUL estimations, a new RUL estimation method is proposed based on an improved UKF in this work. The proposed method is mainly utilized for a special kind of degradation problems in which their monitored measurements have a linear relation with their degradation states. In the proposed method, an improved UKF is constructed firstly based on the KF method and an adaptive strategy. KF is utilized to tackle the linear relationship between the monitored measurements and the degradation states. The adaptive strategy is used to adjust the noise covariance adaptively in the state estimation process. Three degradation problems are analyzed to verify the effectiveness of the proposed method. The results of three cases show that the proposed method can achieve more robust and accurate RUL estimations than the conventional UKF-based method under the uncertainties of the initial parameters. Hence, the proposed method seems a feasible choice for the RUL estimation of many practical engineering problems.

Funding Statement: This work is supported by the National Key R & D Program of China (Grant No. 2018YFB1701400), the National Science Fund for Distinguished Young Scholars (Grant No. 51725502), the Foundation for Innovative Research Groups of the National Natural Science Foundation of China (Grant No. 51621004).

Conflicts of Interest: The authors declare that they have no conflicts of interest to report regarding the present study.

References

1. Javed, K., Gouriveau, R., Zerhouni, N. (2017). State of the art and taxonomy of prognostics approaches, trends of prognostics applications and open issues towards maturity at different technology readiness levels. *Mechanical Systems and Signal Processing, 94,* 214–236. DOI 10.1016/j.ymssp.2017.01.050.
2. Lee, J., Wu, F., Zhao, W., Ghaffari, M., Liao, L. et al. (2014). Prognostics and health management design for rotary machinery systems-reviews, methodology and applications. *Mechanical Systems and Signal Processing, 42(1–2),* 314–334. DOI 10.1016/j.ymssp.2013.06.004.
3. Heng, A., Zhang, S., Tan, A. C., Mathew, J. (2009). Rotating machinery prognostics: state of the art, challenges and opportunities. *Mechanical Systems and Signal Processing, 23(3),* 724–739. DOI 10.1016/j.ymssp.2008.06.009.
4. Wang, D., Tsui, K. L. (2018). Brownian motion with adaptive drift for remaining useful life prediction: revisited. *Mechanical Systems and Signal Processing, 99,* 691–701. DOI 10.1016/j.ymssp.2017.07.015.
5. Kim, N. H., An, D., Choi, J. H. (2016). *Prognostics and health management of engineering systems: an introduction*. New York: Springer.
6. Singleton, R. K., Strangas, E. G., Aviyente, S. (2014). Extended Kalman filtering for remaining-useful-life estimation of bearings. *IEEE Transactions on Industrial Electronics, 62(3),* 1781–1790. DOI 10.1109/TIE.2014.2336616.
7. Lei, Y. (2016). *Intelligent fault diagnosis and remaining useful life prediction of rotating machinery*. Oxford: Butterworth-Heinemann.
8. Miao, Q., Xie, L., Cui, H., Liang, W., Pecht, M. (2013). Remaining useful life prediction of lithium-ion battery with unscented particle filter technique. *Microelectronics Reliability, 53(6),* 805–810. DOI 10.1016/j.microrel.2012.12.004.
9. Wang, D., Yang, F., Tsui, K. L., Zhou, Q., Bae, S. J. (2016). Remaining useful life prediction of lithium-ion batteries based on spherical cubature particle filter. *IEEE Transactions on Instrumentation and Measurement, 65(6),* 1282–1291. DOI 10.1109/TIM.2016.2534258.
10. Johnson, S. B., Gormley, T., Kessler, S., Mott, C., Patterson-Hine, A. et al. (2011). *System health management: with aerospace applications*. Chichester: John Wiley & Sons.

11. Si, X. S., Wang, W., Hu, C. H., Zhou, D. H. (2011). Remaining useful life estimation—a review on the statistical data driven approaches. *European Journal of Operational Research, 213(1),* 1–14. DOI 10.1016/j.ejor.2010.11.018.
12. Si, X. S., Zhang, Z. X., Hu, C. H. (2017). *Data-driven remaining useful life prognosis techniques*. Beijing: National Defense Industry Press and Springer-Verlag GmbH.
13. Chui, C. K., Chen, G. (2017). *Kalman filtering: with real-time applications*. Fifth edition. Cham: Springer International Publishing.
14. Dong, G., Wei, J., Chen, Z. (2016). Kalman filter for onboard state of charge estimation and peak power capability analysis of lithium-ion batteries. *Journal of Power Sources, 328,* 615–626. DOI 10.1016/j.jpowsour.2016.08.065.
15. Qian, Y., Yan, R., Hu, S. (2014). Bearing degradation evaluation using recurrence quantification analysis and Kalman filter. *IEEE Transactions on Instrumentation and Measurement, 63(11),* 2599–2610. DOI 10.1109/TIM.2014.2313034.
16. Plett, G. L. (2004). Extended Kalman filtering for battery management systems of LiPB-based HEV battery packs: part 3. State and parameter estimation. *Journal of Power Sources, 134(2),* 277–292. DOI 10.1016/j.jpowsour.2004.02.033.
17. Bressel, M., Hilairet, M., Hissel, D., Bouamama, B. O. (2016). Extended Kalman filter for prognostic of proton exchange membrane fuel cell. *Applied Energy, 164,* 220–227. DOI 10.1016/j.apenergy.2015.11.071.
18. Pérez, G., Garmendia, M., Reynaud, J. F., Crego, J., Viscarret, U. (2015). Enhanced closed loop state of charge estimator for lithium-ion batteries based on extended Kalman filter. *Applied Energy, 155,* 834–845. DOI 10.1016/j.apenergy.2015.06.063.
19. Wan, E. A., Van Der Merwe, R. (2000). The unscented Kalman filter for nonlinear estimation. *Proceedings of the IEEE 2000 Adaptive Systems for Signal Processing, Communications, and Control Symposium (Cat. No. 00EX373),* pp. 153–158. Canada: Lake Louise, Alberta, IEEE.
20. He, W., Williard, N., Chen, C., Pecht, M. (2014). State of charge estimation for Li-ion batteries using neural network modeling and unscented Kalman filter-based error cancellation. *International Journal of Electrical Power & Energy Systems, 62,* 783–791. DOI 10.1016/j.ijepes.2014.04.059.
21. Chen, K., Yu, J. (2014). Short-term wind speed prediction using an unscented Kalman filter based state-space support vector regression approach. *Applied Energy, 113,* 690–705. DOI 10.1016/j.apenergy.2013.08.025.
22. Djuric, P. M., Kotecha, J. H., Zhang, J., Huang, Y., Ghirmai, T. et al. (2003). Particle filtering. *IEEE Signal Processing Magazine, 20(5),* 19–38. DOI 10.1109/MSP.2003.1236770.
23. Zio, E., Peloni, G. (2011). Particle filtering prognostic estimation of the remaining useful life of nonlinear components. *Reliability Engineering & System Safety, 96(3),* 403–409. DOI 10.1016/j.ress.2010.08.009.
24. Jouin, M., Gouriveau, R., Hissel, D., Péra, M. C., Zerhouni, N. (2016). Particle filter-based prognostics: review, discussion and perspectives. *Mechanical Systems and Signal Processing, 72,* 2–31. DOI 10.1016/j.ymssp.2015.11.008.
25. Santhanagopalan, S., White, R. E. (2010). State of charge estimation using an unscented filter for high power lithium ion cells. *International Journal of Energy Research, 34(2),* 152–163. DOI 10.1002/er.1655.
26. Wan, E. A., Van Der Merwe, R., Haykin, S. (2001). The unscented Kalman filter. *Kalman Filtering and Neural Networks, 5(2007),* 221–280.
27. Xue, H., Chen, B., Wan, J. (2009). A distributed target tracking algorithm based on asynchronous wireless sensor networks. *International Conference on Electronic Computer Technology,* pp. 549–553. China: Macau, IEEE.
28. Sikorska, J. Z., Hodkiewicz, M., Ma, L. (2011). Prognostic modelling options for remaining useful life estimation by industry. *Mechanical Systems and Signal Processing, 25(5),* 1803–1836. DOI 10.1016/j.ymssp.2010.11.018.
29. Chen, K., Laghrouche, S., Djerdir, A. (2019). Fuel cell health prognosis using unscented Kalman filter: postal fuel cell electric vehicles case study. *International Journal of Hydrogen Energy, 44(3),* 1930–1939. DOI 10.1016/j.ijhydene.2018.11.100.
30. Dong, G., Wei, J., Chen, Z., Sun, H., Yu, X. (2017). Remaining dischargeable time prediction for lithium-ion batteries using unscented Kalman filter. *Journal of Power Sources, 364,* 316–327. DOI 10.1016/j.jpowsour.2017.08.040.

31. Tse, P. W., Wang, D. (2017). Enhancing the abilities in assessing slurry pumps' performance degradation and estimating their remaining useful lives by using captured vibration signals. *Journal of Vibration and Control, 23(12),* 1925–1937. DOI 10.1177/1077546315604522.
32. Dolenc, B., Boškoski, P., Stepančič, M., Pohjoranta, A., Juričić, Đ. (2017). State of health estimation and remaining useful life prediction of solid oxide fuel cell stack. *Energy Conversion and Management, 148,* 993–1002. DOI 10.1016/j.enconman.2017.06.041.
33. Wang, D., Yang, F., Zhao, Y., Tsui, K. L. (2017). Prognostics of lithium-ion batteries based on state space modeling with heterogeneous noise variances. *Microelectronics Reliability, 75,* 1–8. DOI 10.1016/j.microrel.2017.06.002.
34. Cui, L., Wang, X., Xu, Y., Jiang, H., Zhou, J. (2019). A novel switching unscented Kalman filter method for remaining useful life prediction of rolling bearing. *Measurement, 135,* 678–684. DOI 10.1016/j. measurement.2018.12.028.
35. Zheng, X., Fang, H. (2015). An integrated unscented Kalman filter and relevance vector regression approach for lithium-ion battery remaining useful life and short-term capacity prediction. *Reliability Engineering & System Safety, 144,* 74–82. DOI 10.1016/j.ress.2015.07.013.
36. Daigle, M., Saha, B., Goebel, K. (2012). A comparison of filter-based approaches for model-based prognostics. *IEEE Aerospace Conference,* pp. 1–10. USA: Big Sky, MT, IEEE.
37. Chang, Y., Fang, H., Zhang, Y. (2017). A new hybrid method for the prediction of the remaining useful life of a lithium-ion battery. *Applied Energy, 206,* 1564–1578. DOI 10.1016/j.apenergy.2017.09.106.
38. Andre, D., Appel, C., Soczka-Guth, T., Sauer, D. U. (2013). Advanced mathematical methods of SOC and SOH estimation for lithium-ion batteries. *Journal of Power Sources, 224,* 20–27. DOI 10.1016/j.jpowsour.2012.10.001.
39. Wang, Y., Binaud, N., Gogu, C., Bes, C., Fu, J. (2016). Determination of Paris' law constants and crack length evolution via extended and unscented Kalman filter: an application to aircraft fuselage panels. *Mechanical Systems and Signal Processing, 80,* 262–281. DOI 10.1016/j.ymssp.2016.04.027.
40. Plett, G. L. (2006). Sigma-point Kalman filtering for battery management systems of LiPB-based HEV battery packs: part 2: simultaneous state and parameter estimation. *Journal of Power Sources, 161(2),* 1369–1384. DOI 10.1016/j.jpowsour.2006.06.004.
41. Zhang, X., Wang, Y., Liu, C., Chen, Z. (2017). A novel approach of remaining discharge energy prediction for large format lithium-ion battery pack. *Journal of Power Sources, 343,* 216–225. DOI 10.1016/j. jpowsour.2017.01.054.
42. Sun, F., Hu, X., Zou, Y., Li, S. (2011). Adaptive unscented Kalman filtering for state of charge estimation of a lithium-ion battery for electric vehicles. *Energy, 36(5),* 3531–3540. DOI 10.1016/j.energy.2011.03.059.
43. Mohamed, A. H., Schwarz, K. P. (1999). Adaptive Kalman filtering for INS/GPS. *Journal of Geodesy, 73(4),* 193–203. DOI 10.1007/s001900050236.
44. Fan, J., Yung, K. C., Pecht, M. (2013). Prognostics of chromaticity state for phosphor-converted white light emitting diodes using an unscented Kalman filter approach. *IEEE Transactions on Device and Materials Reliability, 14(1),* 564–573. DOI 10.1109/TDMR.2013.2283508.
45. Tian, Y., Xia, B., Sun, W., Xu, Z., Zheng, W. (2014). A modified model based state of charge estimation of power lithium-ion batteries using unscented Kalman filter. *Journal of Power Sources, 270,* 619–626. DOI 10.1016/j. jpowsour.2014.07.143.
46. Julier, S. J., Uhlmann, J. K. (2004). Unscented filtering and nonlinear estimation. *Proceedings of the IEEE, 92(3),* 401–422. DOI 10.1109/JPROC.2003.823141.
47. He, W., Williard, N., Chen, C., Pecht, M. (2013). State of charge estimation for electric vehicle batteries using unscented Kalman filtering. *Microelectronics Reliability, 53(6),* 840–847. DOI 10.1016/j.microrel.2012.11.010.
48. Zuluaga, C. D., Alvarez, M. A., Giraldo, E. (2015). Short-term wind speed prediction based on robust Kalman filtering: an experimental comparison. *Applied Energy, 156,* 321–330. DOI 10.1016/j.apenergy.2015.07.043.
49. Auger, F., Hilairet, M., Guerrero, J. M., Monmasson, E., Orlowska-Kowalska, T. et al. (2013). Industrial applications of the Kalman filter: a review. *IEEE Transactions on Industrial Electronics, 60(12),* 5458–5471. DOI 10.1109/TIE.2012.2236994.

50. An, D., Choi, J. H., Kim, N. H. (2013). Prognostics 101: a tutorial for particle filter-based prognostics algorithm using Matlab. *Reliability Engineering & System Safety, 115,* 161–169. DOI 10.1016/j.ress.2013.02.019.
51. Celaya, J. R., Kulkarni, C. S., Biswas, G., Goebel, K. (2012). Towards a model-based prognostics methodology for electrolytic capacitors: a case study based on electrical overstress accelerated aging. *International Journal of Prognostics and Health Management, 3(2),* 33.
52. Celaya, J., Kulkarni, C., Biswas, G., Goebel, K. (2012). *Capacitor electrical stress data set-2, NASA ames prognostics data repository*. Moffett Field, CA: NASA Ames Research Center.
53. Eker, Ö. F., Camci, F., Jennions, I. K. (2012). Major challenges in prognostics: study on benchmarking prognostic datasets, *European Conference of Prognostics and Health Management Society, Germany*: *Dresden,* pp. 1–8.
54. Goebel, K. F. (1996). *Management of uncertainty in sensor validation, sensor fusion, and diagnosis of mechanical systems using soft computing techniques,* Berkeley, CA: University of California.
55. Agogino, A., Goebel, K. (2007). *Milling data set, NASA ames prognostics data repository*. Moffett Field, CA: NASA Ames Research Center.